Journal of Microencapsulation
Publication details, including instructions for authors and subscription information:
http://www.informaworld.com/smpp/title~content=t713723933

Co-encapsulation of dexamethasone 21-acetate and SPIONs into biodegradable polymeric microparticles designed for intra-articular delivery

Nicoleta Butoescu [a]; Olivier Jordan [a]; Alke Petri-Fink [b]; Heinrich Hofmann [b]; Eric Doelker [a]
[a] School of Pharmaceutical Sciences, University of Geneva, University of Lausanne, Geneva, Switzerland [b] Powder Technology Laboratory, Ecole Polytechnique Fédérale de Lausanne (EPFL), Lausanne, Switzerland

First Published:2008

To cite this Article Butoescu, Nicoleta, Jordan, Olivier, Petri-Fink, Alke, Hofmann, Heinrich and Doelker, Eric(2008)'Co-encapsulation of dexamethasone 21-acetate and SPIONs into biodegradable polymeric microparticles designed for intra-articular delivery',Journal of Microencapsulation,25:5,339 — 350
To link to this Article: DOI: 10.1080/02652040801999551
URL: http://dx.doi.org/10.1080/02652040801999551

Journal of Microencapsulation, August 2008; 25(5): 339–350

informa
healthcare

Co-encapsulation of dexamethasone 21-acetate and SPIONs into biodegradable polymeric microparticles designed for intra-articular delivery

NICOLETA BUTOESCU[1], OLIVIER JORDAN[1], ALKE PETRI-FINK[2], HEINRICH HOFMANN[2], & ERIC DOELKER[1]

[1]*School of Pharmaceutical Sciences, University of Geneva, University of Lausanne, Geneva, Switzerland, and*
[2]*Powder Technology Laboratory, Ecole Polytechnique Fédérale de Lausanne (EPFL), Lausanne, Switzerland*

(Received 14 December 2007; accepted 18 February 2008)

Abstract
Objective: Intra-articular drug delivery systems still suffer from too short-lasting effects. Magnetic particles retained in the joint using an external magnetic field might prolong the local release of an anti-inflammatory drug. For the purpose, superparamagnetic iron oxide nanoparticles (SPIONs) and dexamethasone 21-acetate (DXM) were co-encapsulated into biodegradable microparticles.
Methods: Poly(D,L-lactide-*co*-glycolide) microparticles embedding both SPIONs and DXM were prepared by a double emulsion technique. The formulation was optimized in two steps, a screening design and a full factorial design, aiming at 10-μm particle diameter and high DXM encapsulation efficacy.
Results: The most significant parameters were the polymer concentration, the stirring speed during solvent extraction and the extractive volume. Increasing the polymer concentration from 200 to 300 mg ml^{-1}, both the microparticle mean diameter and the DXM encapsulation efficacy increased up to 12 μm and 90%, respectively. The microparticles could be retained with an external magnet of 0.8 T placed at 3 mm. Faster DXM release was obtained for smaller microparticles.
Conclusion: The experimental set-up offered the tools for tailoring a formulation with magnetic retention properties and DXM release patterns corresponding to the required specifications for intra-articular administration.

Keywords: *Magnetic microparticles, dexamethasone, experimental design, drug release, superparamagnetic iron oxide nanoparticles (SPION)*

Introduction

Rheumatic diseases, such as arthritis or osteoarthritis, are severe conditions characterized by joint inflammation and cartilage erosion, respectively, leading in both cases to a gradual loss of the mobility of the patients and to an impairment of their quality of life. Regarding the treatment of these affections, two main approaches are generally adopted: the use of symptomatic drugs aiming at pain relief and that of drugs fighting against the cause of the disease, when known. Anti-inflammatory drugs, both non-steroidal and steroidal, belong to the first category. However, they are usually short-acting substances, requiring repeated administration at high doses, resulting in severe systemic side effects. In this respect, longer-acting medications, generally corticosteroids (Gaffney et al. 1995; Raynauld et al. 2003) administered by intra-articular injections, have represented a major breakthrough in the treatment of arthritis or osteoarthritis (Gerwin et al. 2006). Clinical tests have shown, however, that intra-articular corticosteroids, despite their net efficacy, are not devoid of side effects. For example, because of their crystalline structure, a condition referred to as crystal-induced arthritis was described in 10% of the patients receiving an intra-articular injection (Tosu 1992; Moore 2005). Moreover, due to lymph drainage (Gerwin et al. 2006) or macrophage uptake, the residence time of corticosteroid molecules in the joint is very small, requiring frequent intra-articular injections in order to obtain a sustained

Correspondence: Eric Doelker, School of Pharmaceutical Sciences, University of Geneva, 30 Quai Ernest-Ansermet, Sciences II, 1211 Geneva 4, Switzerland. Tel: +41223796148. Fax: +41223796567. E-mail: eric.doelker@pharm.unige.ch

ISSN 0265–2048 print/ISSN 1464–5246 online
DOI: 10.1080/02652040801999551

clinical result. The complications of such frequent injections in terms of infections or joint instability, although rare, remain severe (Moore 2005). All these aspects emphasize the need to develop drug delivery systems allowing the sustained release of the active substance in order to reduce the frequency of the intra-articular injections together with the related potential deleterious effects.

In this respect, drug delivery systems, such as liposomes (Metselaar et al. 2006), nano- and microparticles (Tuncay et al. 2000; Bozdag et al. 2001; Horisawa et al. 2002a), all embedding anti-inflammatory substances, have been designed for intra-articular administration in the attempt to reduce the systemic side effects observed after the oral or i.v. administration of the respective anti-inflammatory substances. However, the efficacy of these vectors was hindered by the fact that they were rapidly cleared out of the joint.

Magnetic microparticles loaded with corticosteroids could represent a valuable way of addressing all the above-mentioned issues. First, because the drug is present in a solubilized form in the joint, the deleterious crystal-induced pain could be avoided. Secondly, due to their magnetic nature, these systems could be retained in the joint with an external magnetic field, resulting in an increased residence time in the articular cavity, allowing the active substance to be released and to act locally. Superparamagnetic iron oxide nanoparticles (SPIONs) can be used as magnetic material. Their biocompatibility with the tissues of the joint, notably with the synovial membrane, was shown by Schultze et al. (2005) in sheep. Moreover, these magnetic nanoparticles are already used in humans as superparamagnetic contrast agents (Kopp et al. 1997) and are thus expected to produce neither immunogenic nor inflammatory reactions.

The aim of this study was thus to formulate biodegradable magnetic microparticles for intra-articular delivery of the anti-inflammatory steroid dexamethasone 21-acetate (DXM). The choice of this ester was based on previous studies. It could be demonstrated (results not shown) that the use of dexamethasone sodium phosphate was not possible, due to its reaction with the free iron ions, leading to precipitation in the internal aqueous phase, nor was it possible to use dexamethasone base, due to the formation of dexamethasone crystals, limiting its encapsulation efficacy. The formation of dexamethasone crystals in this case has already been reported by Gomez-Gaete et al. (2007). Few studies have been published regarding the separate encapsulation of dexamethasone or of SPIONs into polymeric particles (Beck et al. 2007; Okassa et al. 2007). Concerning the encapsulation of both dexamethasone and SPIONs into microparticles, the only report is that of Ghassabian et al. (1996) who prepared dexamethasone sodium phosphate-containing magnetic albumin microspheres by an emulsion in cottonseed oil. These particles showed a very rapid release pattern, all substance being released within 3 h. Moreover, the studies mentioning the co-encapsulation of SPIONs and another drug are also few, proving that research in this domain is still at the initial stage. Cheng et al. (2006) prepared magnetic PLGA microparticles for the oral delivery of insulin. Magnetic PLLA nanoparticles encapsulating chemotherapeutic drugs, suitable for tumour imaging and drug delivery, were formulated by Hamoudeh et al. (2007), but also by Hu et al. (2006). Poly(ε-caprolactone) magnetic nanoparticles containing cisplatin or gemcitabime were also prepared (Yang et al. 2006). Timko et al. (2006) encapsulated indomethacin into poly(D, L-lactide) magnetic nanoparticles for magnetic drug targeting (Zavisova et al. 2007).

Although some magnetic microparticles have already been prepared for magnetically triggered oral delivery, imaging or magnetic drug targeting, to the authors' knowledge there is no example in the literature of magnetic particles intended for intra-articular delivery. The requirements for intra-articular magnetic retention are actually distinct from these above applications. To ensure a maximum retention efficacy, one needs to maximize the balance between magnetic and viscous forces, thus aiming at sufficiently large particles. One also aims at injecting only small quantities of iron oxide to the joint, still ensuring magnetic particle retention, while limiting the possible side effects due to large iron oxide content (Weissleder et al. 1989).

Concerning the intra-articular administration, the literature provides little information on the most suitable particle size. In this respect, various research teams have studied microparticles with mean diameters ranging from the nanometer scale up to 200–300 μm (Ratcliffe et al. 1987; Horisawa et al. 2002a,b, Liggins et al. 2004). It has been demonstrated that particles with mean diameters of more than 20 μm are not captured by synoviocytes and macrophages, while smaller microparticles can be internalized. The process of internalization could however be of great importance if the targeted substance needs to act intra-cellularly, such as corticosteroids, which have nuclear receptors. Based on all these studies and in view of future clinical applications, one considers that the most useful size would be ~10 μm in order to limit the possible inflammatory reactions in the articular joint (Horisawa et al. 2002b). Concerning the biodegradable polymer matrix of the microparticles, many materials have been investigated for the intra-articular administration: poly(lactic acid), poly(butyl cyanoacrylate), gelatin, albumin, polycaprolactone, DL-lactide/glycolide copolymer (Ratcliffe et al. 1987; Horisawa et al. 2002a,b, Liggins et al. 2004). Due to its biocompatibility and wide acceptance, DL-lactide/glycolide copolymer (PLGA) was chosen as the microparticle matrix.

Practically, the corticosteroid dexamethasone 21-acetate and SPIONs, as ferrofluid, were

co-encapsulated into PLGA biodegradable microparticles and the formulation process was optimized by means of the experimental design approach. First of all, in order to identify the most relevant parameters affecting the formulation process, a screening design was performed. Afterwards, varying only the most relevant parameters, an optimization design was performed in order to find the best conditions leading to the highest DXM loading correlated with the highest encapsulation efficacy. Microparticles were characterized in terms of size, DXM loading and DXM encapsulation efficacy, SPION content and, last but not least, magnetic retention and DXM release patterns.

Materials and methods

Materials

Poly(D,L-lactide-co-glycolide) (PLGA 75:25, inherent viscosity 0.2 dl g^{-1}) was provided by Boehringer Ingelheim (Germany) (Resomer® RG 752S). Dexamethasone 21-acetate was purchased from Sigma Aldrich (Switzerland). Poly(vinyl alcohol) (PVA) was a gift from Clariant GmbH (Germany) (Mowiol® 4-88, hydrolysis degree 88% and molecular weight of 26 kDa). SPIONs were prepared according to the method described by Chastellain et al. (2004). They were used in the process as a suspension, referred to as ferrofluid, with an iron content of 10.3 mg ml^{-1}, as assessed by atomic absorption. Ethyl acetate, acetonitrile and ethanol were of analytical grade. The purified water used during the experiments was obtained with a MilliQ system (Millipore, Switzerland).

Preparation of microparticles

The microparticles were prepared by a double emulsion-solvent extraction method. Briefly, 1 ml of organic phase containing either 200, 250 or 300 mg ml^{-1} RG 752S and 10 mg ml^{-1} DXM in ethyl acetate added with 10% ethanol as a co-solvent (DXM solubility in the solvent mixture is 19 mg ml^{-1}, as determined by HPLC) was emulsified with 0.15 ml of ferrofluid (10 mg ml^{-1} iron) by means of a sonicator for 10 s (VibraCell™ VC 50T, Sonics and Materials, USA). This primary emulsion was emulsified with 2 ml 2% PVA solution using a T25 Ultra-Turrax (IKA Labortechnik, Germany) for 1 min at 8000 rpm. This final emulsion was then poured into 10, 15 or 20 ml of water and mechanically stirred for 4 h at room temperature at 400, 700 or 1000 rpm (Eurostar Digital, IKA labortechnik, Germany). The resulting microparticles were separated by using a Jouan BR 3.11 centrifuge (IG, Switzerland), washed 3 times with MilliQ water, freeze-dried (Modulyo Freeze Dryer, Edwards, Switzerland) and finally stored at 4°C.

Note that the values of the above-mentioned technological parameters were those used in the full factorial design, performed after the screening design. During the screening design, more factors were varied, notably PLGA concentration, ferrofluid volume, external aqueous phase volume, PVA concentration in the external aqueous phase, stirring speed and stirring time during the final emulsification step and extractive volume. The low and high levels of these nine factors are presented in Table I. Among these nine factors, three of them turned out to be relevant to the formulation process and, hence, they were subsequently used in the full factorial design. The low levels and the high levels of these three factors are presented in Table II.

Microparticle characterization

Size measurements were performed using light scattering (Mastersizer S, Malvern, UK) after dispersing the particles in water and the sizes were expressed as D[4;3].

Scanning electron microscopy was performed on gold-coated freeze-dried samples (Balzers SCD 004 Sputter Coater) with a JEOL JSM-6400 microscope (Tokyo, Japan) at an accelerating voltage of 10–15 kV in order to determine the surface morphology of the particles.

Table I. Parameters of the screening design with their low and high levels.

Factor	Low level	High level
PLGA concentration (mg ml^{-1})	200	300
Ferrofluid volume (ml)	0.10	0.20
External aqueous phase volume (ml)	2	4
PVA concentration in external aqueous phase (%)	2	5
Stirring speed during final emulsification step (rpm)	8000	9750
Stirring time during final emulsification step (min)	1	2
Extractive volume (ml)	10	20
PVA concentration in extraction medium (%)	0	0.60
Stirring speed during solvent extraction step (rpm)	400	1000

Table II. Factors of the full factorial design with their low and high levels.

Factor	Low level	High level
PLGA concentration (mg ml^{-1})	200	300
Stirring speed during solvent extraction step (rpm)	400	1000
Extractive volume (ml)	10	20

Magnetic retention of the microspheres was assessed using the device depicted in Figure 1 and equipped with a Nd-Fe-B magnet generating a magnetic field of 0.8 T. The percentage of retained microspheres was calculated by dividing the final microparticle mass (after discarding the remaining suspension and freeze-drying the tube content) by the initial one.

DXM content of the microparticles was measured by HPLC, using a 100-5 C18 Nucleosil column (250/4.6, Macherey Nagel), an acetonitrile:water 1:1 mobile phase, a flow rate of $0.8\,\mathrm{ml\,min^{-1}}$ and detection at 254 nm, after solubilization of the particles in acetonitrile. The suspension was centrifuged at 21 000 rpm in order to separate the insoluble SPIONs from the DXM-containing solution.

The DXM encapsulation efficacy and DXM loading into the microparticles were calculated based on the following equations:

$$\text{DXM encapsulation efficacy} = \frac{wt\,\text{DXM entrapped}}{wt\,\text{DXM used}} \cdot 100 \quad (1)$$

$$\text{DXM loading} = \frac{wt\,\text{DXM entrapped}}{wt\,\text{microparticles used for dosing}} \cdot 100 \quad (2)$$

The solid mass obtained after microparticle dissolution in acetonitrile was then used to assess the SPION content. This was determined by a spectrophotometric method based on the formation of a red complex between Fe^{+3} and o-phenanthroline. Briefly, the solid was left to dry overnight and then treated with 6 M HCl in order to solubilize Fe_3O_4. An aliquot of this solution was taken and treated with 1% hydroxylamine hydrochloride aqueous solution to reduce Fe^{3+} ions into Fe^{2+}. A $200\,\mathrm{g\,L^{-1}}$ sodium acetate solution was then added and finally 0.015 M o-phenanthroline hydrochloride solution was added in order to obtain the red complex. The absorbance was immediately measured at 510 nm using a spectrophotometer.

DXM release kinetics was conducted by placing 10–15 mg of microparticles in 50 ml 15 mM PBS pH 7.4 with 2 mM sodium azide as a preservative agent and 0.5% polysorbate 80, to increase the solubility of DXM and the wettability of the microparticles (DXM solubility in the release medium is $0.042\,\mathrm{mg\,ml^{-1}}$, as determined by HPLC). The quantity of particles was adjusted in order to have sink conditions during the duration of the experiment. The suspension was continuously horizontally shaken at 120 rpm and 37°C in a GFL-3033 shaker (Burgwedel, Germany). At defined time intervals, aliquots of 0.5 ml were withdrawn, centrifuged in order to separate microparticles, which were returned to the release medium, and assayed for DXM using HPLC. The withdrawn volume was replaced by fresh PBS. All experiments were performed in triplicate.

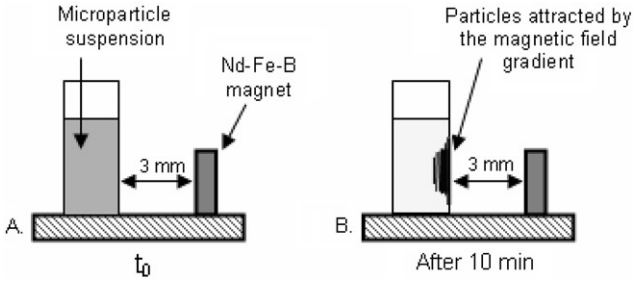

Figure 1. Apparatus for the assessment of microparticle magnetic retention.

Screening design

In order to determine the influence of the most relevant factors on microparticle size, DXM loading and DXM encapsulation efficacy, a screening design was performed. The factors of the design were chosen based on preliminary experiments and bibliography data. A Plackett-Burman matrix was used to study the influence of nine factors in 12 experiments (Khan et al. 2000). In order to estimate the variability of the experimental results, four centre points were added to the design. The number of the degrees of freedom available to estimate the error was six. The set-up was completely randomized, in order to minimize the effect of possible disruptive variables. The low levels and the high levels of the parameters studied in this experimental design are presented in Table I. The studied PLGA concentrations varied between 200–300 $\mathrm{mg\,ml^{-1}}$, because, based on preliminary experiments, these values allowed one to obtain microparticles with a diameter ~10 μm and a high DXM encapsulation efficacy. Moreover, another reason for selecting these PLGA concentrations was the ratio of polymer:DXM. In order to ensure a sufficient DXM solubility in the organic phase, a maximal polymer concentration of $300\,\mathrm{mg\,ml^{-1}}$ was set, resulting in microparticles with DXM loading suitable for future i.a. clinical applications. On the other hand, if polymer concentration is below $200\,\mathrm{mg\,ml^{-1}}$, microparticle size is in the range of nanometer scale, which hinders the encapsulation of an optimal SPION quantity. Besides PLGA concentration, eight other factors were screened in order to determine the best conditions leading to the highest DXM encapsulation efficacy combined with the highest DXM loading. The studied ferrofluid volume varied between 0.1–0.2 ml, which represented 10–20% of the organic phase, these being the most common ratios between the internal aqueous and organic phases. The external aqueous phase volume, the PVA concentration in the external aqueous phase, the stirring speed and the time during the final emulsification step were chosen based on the preliminary experiments. The volume of the extraction aqueous phase

was between 10–20 ml, because at the beginning of the double emulsion, droplets need to harden progressively in order to avoid precipitation of the DXM out of the microparticles. After 10 min, the same extraction aqueous medium was added to a final extractive volume of 50 ml for all experiments. This suspension was then stirred for 4 h, for complete solvent evaporation. All the conditions of the 16 batches of the screening design are presented in Table III.

Factorial design

The screening design was a means to identify the most significant factors in the process and to rank them from the point of view of their importance on the microparticle formulation. Subsequently, a full factorial design was carried out aiming at optimizing the formulation with respect to these sole factors. A group of eight experiments was designed and two centre points were added in order to estimate the experimental error. In a similar manner as for the screening design, the three factors had a high and a low level (Table II). The plan was completely randomized and the sequence of runs is presented in Table IV.

In both the screening and the factorial designs, the responses considered were: DXM loading, DXM encapsulation efficacy and microparticle size. Data were treated using the StatGraphics^{TM} software. Here, in order to define the optimal conditions for the microparticle formulation process, the approach of maximization of a desirability function was chosen. The desirability function method is based on that fact that a process is acceptable only if all its quality characteristics are between the limits of acceptability. The acceptable limits of the quality characteristics of our process are listed in Table V.

From these designs, one could determine the 'most desirable' experiment from the point of view of the microparticle size, DXM loading and DXM encapsulation efficacy. Nevertheless, additional criteria were considered for the selection of the final formulation, namely SPION content, magnetic retention and DXM release.

Results and discussion

Screening design

The screening design has been carried out to determine the order of significance of the nine parameters for the microparticle formulation. The standardized Pareto charts presented in Figures 2–4 show the estimated effects of the parameters on the response variables in descending order of their importance. The length of each bar is proportional to the standardized effect, which is equal to the estimated effect divided by the standard error. The vertical line delimits which parameters are significant at a confidence level of 95%. It is important to notice that the experimental data fits the mathematical model well for all three studied response variables, with R^2 values of 0.9040, 0.9392 and 0.8324 and adjusted R^2 for the degrees of freedom of the error with values of 0.7602, 0.8481 and 0.5810, respectively, for DXM loading, DXM encapsulation efficacy and particle size.

The significant parameters on DXM loading are, in decreasing order, the extractive volume, PLGA concentration, stirring speed during the extraction step and the external aqueous phase volume, as depicted in Figure 2. All the other parameters are not significant at a confidence level of 95%. The extractive volume has a positive effect on DXM loading, meaning that when the extracting volume increases, the DXM loading increases. In fact, a larger extractive volume can lead to a more rapid diffusion of the solvent out of the microparticles, resulting in earlier microparticle hardening, with increased DMX entrapping efficiency.

Increasing the PLGA concentration in the organic phase from 200 to 300 mg ml^{-1} results in the decrease of the DXM loading due to a lower PLGA:DXM ratio, the DXM concentration in the organic phase remaining constant for all experiments (10 mg ml^{-1}). The increase in the stirring speed during the extraction step leads to increased DXM loading into the microparticles. One possible explanation could also be the more rapid and efficient hardening of microparticles when a higher stirring speed is applied. The fourth significant factor on the DXM loading is the external aqueous phase volume. Indeed, an augmentation in the DXM loading is observed when the external aqueous phase volume augments, which is also related to rapid microparticle hardening.

Regarding the influence of the studied parameters on DXM encapsulation efficacy, the same four parameters as for DXM loading appear to be significant according to Figure 3. The only difference compared to DXM loading is their respective order, the most important factor being PLGA concentration in the organic phase. Figure 3 shows that increasing PLGA concentration results in an increase in DXM encapsulation efficacy. This can be related to the fact that increasing PLGA concentration has the consequence that the DXM molecules are surrounded by more polymer macromolecules, leading to better encapsulation.

The concentration of PLGA in the organic phase has a positive influence on the particle size. The presence of a higher PLGA concentration in the organic phase leads to a higher viscosity, producing larger and more stable primary emulsion droplets. An increase in microparticle size is also related to an increase in the external aqueous phase volume, according to Figure 4. This result is in accordance with previous works, reporting an increase in microparticle size with the external aqueous phase volume (Pean et al. 1998). One possible explanation would be that a larger external aqueous phase volume added to the same

Table III. Parameters of the screening setup and the responses registered for each experiment.

Batch N°	PLGA concentration ($mg\,ml^{-1}$)	Ferrofluid volume (ml)	External aqueous phase volume (ml)	PVAL concentration in external aqueous phase (%)	Stirring speed during final emulsification (rpm)	Stirring time during final emulsification (min)	Extractive volume (ml)	Stirring speed during solvent extraction (rpm)	PVAL concentration in extraction phase (%)	Results		
										Size (μm)	DXM loading (mg%)	DXM encapsulation efficacy (%)
1	200	0.10	4	2.0	9500	2.0	10	1000	0.6	4.4	2.7	56.1
2	200	0.20	2	2.0	8000	2.0	20	1000	0	4.4	2.9	61.0
3	250	0.15	3	3.5	8750	1.5	15	700	0.3	4.5	2.4	62.1
4	200	0.20	2	5.0	9500	1.0	10	400	0.6	2.2	1.8	38.0
5	300	0.10	4	5.0	8000	2.0	10	400	0	11.3	2.2	68.4
6	200	0.10	2	2.0	8000	1.0	10	400	0	5	2.5	51.4
7	300	0.20	4	2.0	8000	1.0	10	1000	0.6	20.7	2.3	72.1
8	200	0.10	4	5.0	9500	1.0	20	1000	0	4	3.6	74.6
9	200	0.20	4	5.0	8000	2.0	20	400	0.6	3.6	3.0	61.9
10	250	0.15	3	3.5	8750	1.5	15	700	0.3	4.4	2.3	60.2
11	250	0.15	3	3.5	8750	1.5	15	700	0.3	5.3	2.6	66.8
12	300	0.10	2	5.0	8000	1.0	20	1000	0.6	6	2.5	78.7
13	300	0.20	4	2.0	9500	1.0	20	400	0	10.4	2.3	71.3
14	250	0.15	3	3.5	8750	1.5	15	700	0.3	5	2.5	63.7
15	300	0.10	2	2.0	9500	2.0	20	400	0.6	5.3	2.4	73.6
16	300	0.20	2	5.0	9500	2.0	10	1000	0	4.1	2.2	67.5

Table IV. Full factorial design and the results for the 10 trials.

Batch N°	PLGA concentration ($mg\,ml^{-1}$)	Stirring speed during solvent extraction (rpm)	Extractive volume (ml)	Results		
				Size (μm)	DXM encapsulation efficacy (%)	DXM loading (mg%)
17	200	400	10	4.2	71.8	3.4
18	300	1000	10	11.9	83.8	2.7
19	200	1000	20	4.8	86.7	4.1
20	300	1000	20	12.0	89.5	2.9
21	200	1000	10	4.8	75.3	3.6
22*	250	700	15	5.5	82.5	3.1
23	250	700	15	5.7	81.5	3.0
24	200	400	20	5.5	80.7	3.8
25	300	400	10	12.6	84.7	2.7
26	300	400	20	12.7	87.3	2.8

*Represents the experience which had the highest value for the desirability function.

Table V. The acceptable characteristics for the response variables studied in the full factorial design.

Response	Objective
DXM encapsulation efficacy	Maximal
DXM loading	Maximal
Particle size	About 10 μm

volume of organic phase results in a decrease in the stirring efficacy, leading to coarser emulsion droplets, which will harden into larger microparticles.

As a result of the screening experiment, the three significant parameters—notably PLGA concentration, external aqueous phase volume, stirring speed during emulsification—were retained for the subsequent optimization study.

Factorial design

The effects of the three retained parameters and their interactions were then investigated in more detail using a full factorial design. The three factors (PLGA concentration, extractive volume and stirring speed during the emulsification step) were varied, while all others were kept at the constant values quoted in the Materials and methods section. On examination of Table IV, it is observed that the microparticle size can be increased up to 3 times when increasing the PLGA concentration from 200 to $300\,mg\,ml^{-1}$. The encapsulation efficacy of DXM for all 10 batches was greater than 70% and due to optimization, DXM loading could be increased by almost 50%.

The results obtained from the full factorial design for the microparticle size confirms that only the PLGA concentration has a significant effect at the 95% confidence level (Figure 5): at higher PLGA concentrations, the particle size increases, demonstrated also by the SEM photomicrographs of Figure 6. From these pictures, one can also see that the microparticles are spherical, quite homogeneous in size, with a non-porous surface. Moreover, the inner structure of the microparticles was studied also by SEM and the image can be seen in Figure 7. By analysing this image, one can conclude that the microparticles do not have a porous inner structure. Some of the particles are empty (capsules) and others have only a few small cavities, but no relationship between the size and the inner structure could be established.

As for the DXM encapsulation efficacy, the most significant factors are the PLGA concentration in the organic phase and the volume of the extracting phase (Figure 5). Moreover, at the 95% confidence level, two interactions are also significant, as depicted in Figure 8, meaning that the effect of each of the two interactive factors is dependent on the level of the other one. In particular, from Figure 8(a) it can be inferred that at 400 rpm, the DXM encapsulation efficacy increases more steeply when PLGA concentration changes from 200 to $300\,mg\,ml^{-1}$ than at 1000 rpm. As for the interaction between the PLGA concentration and the extracting volume, Figure 8(b) shows that when using 10 ml extracting volume, the DXM encapsulating efficacy increases more rapidly when PLGA concentration augments from 200 to $300\,mg\,ml^{-1}$ than when using 20 ml extracting volume.

Regarding DXM loading, two out of the three factors have a significant effect: PLGA concentration and extracting volume (Figure 5). Actually, by increasing the PLGA concentration, a decrease in the DXM loading is noted, due to the fact that the DXM concentration in the organic phase remains the same because of its limited solubility, while the PLGA concentration augments.

Finally, by using the StatGraphics^{TM} software, a multi-response optimization was performed, based on the maximization of a desirability function. This procedure allows the determination of the combination of parameters that optimize all three of the studied responses at the same time. The maximum for the

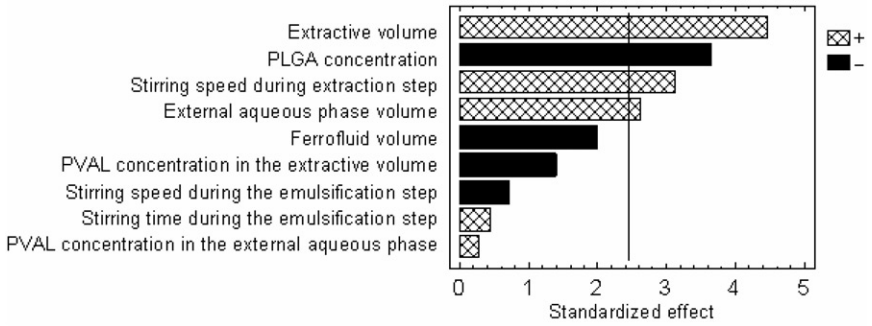

Figure 2. Standardized Pareto chart for DXM loading after the screening design (vertical bar represents $\alpha = 0.05$).

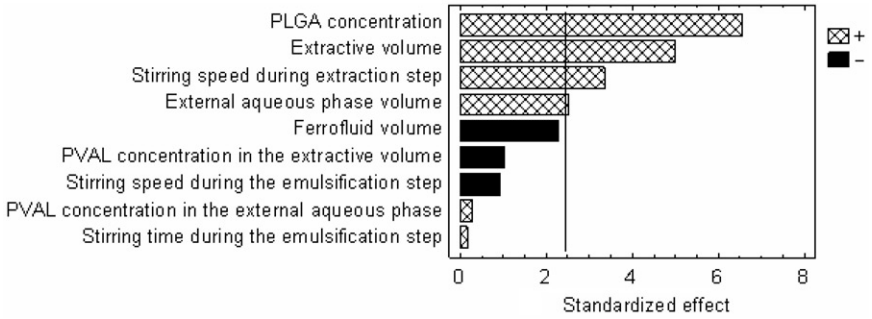

Figure 3. Standardized Pareto chart for DXM encapsulation efficacy after the screening design (vertical bar represents $\alpha = 0.05$).

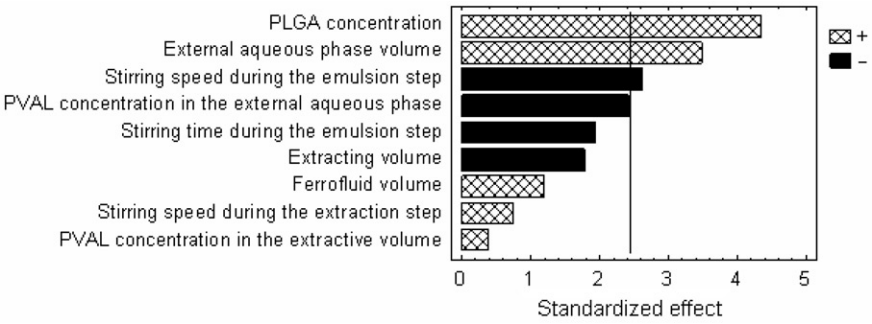

Figure 4. Standardized Pareto chart for size after the screening design (vertical bar represents $\alpha = 0.05$).

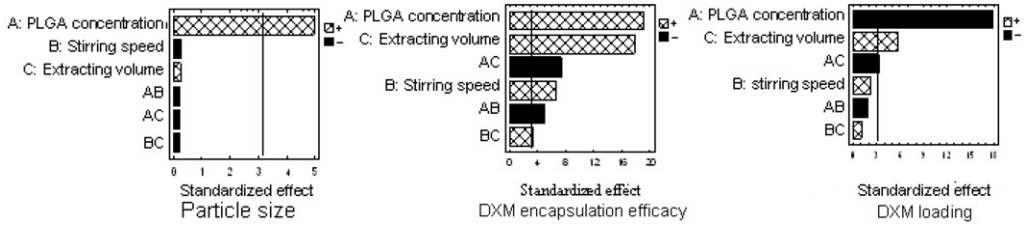

Figure 5. Standardized Pareto charts for the retained responses after the full factorial design (vertical bar represents $\alpha = 0.05$).

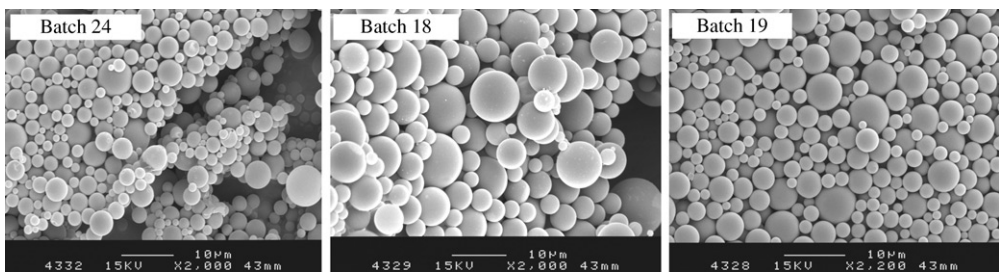

Figure 6. SEM photomicrographs of microparticles of three batches of the full factorial design.

desirability function is obtained for Batch N° 22 of the full factorial design, the characteristics of which are in agreement with the requirements (maximal DXM loading and DXM encapsulation efficacy), except for the microparticle size, which is rather small (5.5 μm), compared with the target value of 10 μm.

SPION encapsulation efficacy and magnetic retention

Together with DXM, SPIONs (used as ferrofluid) were encapsulated into the microparticles. In the screening set-up, three volumes of ferrofluid were studied in the different experiments: 0.10, 0.15 and 0.20 ml (Table III), corresponding to concentrations between 0.45–1.32% of Fe_3O_4 into the microparticles, according to the different possible combinations of the experimental design. It was demonstrated that this parameter is not significant either for the microparticle size or the DXM encapsulation efficacy and loading. Therefore, a volume of 0.15 ml was chosen for the full factorial design, in order to make the microparticles as magnetic as possible, while not using too high of an organic phase:internal aqueous phase (ferrofluid) ratio. The encapsulated Fe_3O_4 into the batches was assessed by the spectrophotometric method with o-phenanthroline and the encapsulation efficacy was calculated. High encapsulation efficacies were obtained both for the batches of the screening design and those of the full factorial design, with values above 70% in all cases, corresponding to iron oxide concentration values between 0.3–0.9% in the microparticles.

For future intra-articular applications, it is important that the microparticles be highly retained by an external magnetic field when the SPION content is minimal, in order to avoid possible toxic effects related to high iron concentrations (Weissleder et al. 1989). As depicted in Figure 9(a), the magnetic retention of all microparticle batches increases with the time of exposure to the magnetic field. After 3 min of exposure, the percentage of retained microparticles is rather small, with values generally not exceeding 50%. The size of the retained

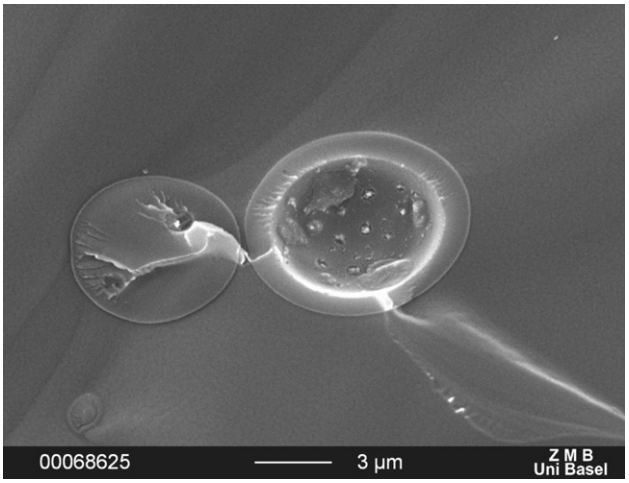

Figure 7. Scanning electron photomicrographs of the Batch 19 showing the inner structure of the microparticles.

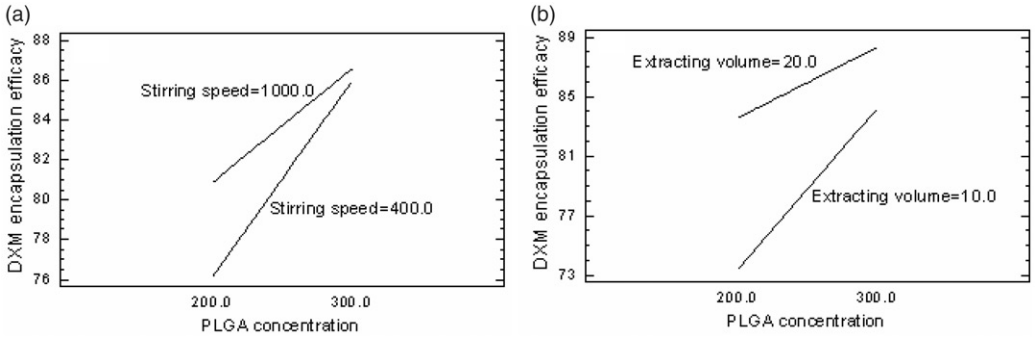

Figure 8. The significant interactions ($\alpha = 0.05$) between the PLGA concentration and the stirring speed (a) and the extracting volume (b), respectively, in the case of DXM encapsulation efficacy.

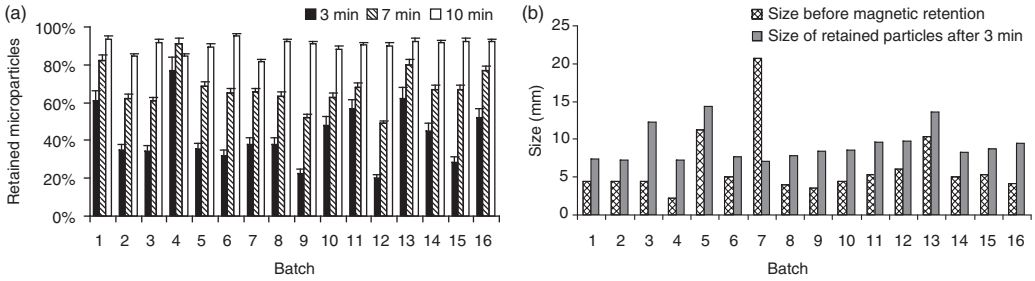

Figure 9. (a) Magnetic retention of microparticle batches of the screening design after 3, 7 and 10 min under the action of a 0.8 T magnetic field; (b) Microparticle size before and after 3 min magnetic retention.

microparticles was measured by light scattering and compared to the initial microparticle size of each batch. From Figure 9(b), it can be observed that after 3 min of retention, only the largest microparticles become retained. This is in agreement with a retention force proportional to the amount of encapsulated SPION and thus, to the particle volume. After 7 min of retention a higher fraction of microparticles are retained, reaching 100% after 10 min of retention for all batches. This result is important in the context of future clinical applications, for which a high retention after a short period of time could guarantee the permanence of the microparticles in the joint, where the active substance could be gradually and locally released. Furthermore, a small amount of SPIONs is sufficient to this end, thus limiting the total iron to be administered.

The same conclusions can be drawn for the batches of the full factorial design, for which the retention of the microparticles also increased with the exposure time to the magnetic field (results not shown).

In order to assess the distribution of SPIONs in the microparticles, TEM was performed. From Figure 10, it can be seen that the iron oxide nanoparticles, corresponding to the dark dots in the microparticle, are quite homogeneously distributed.

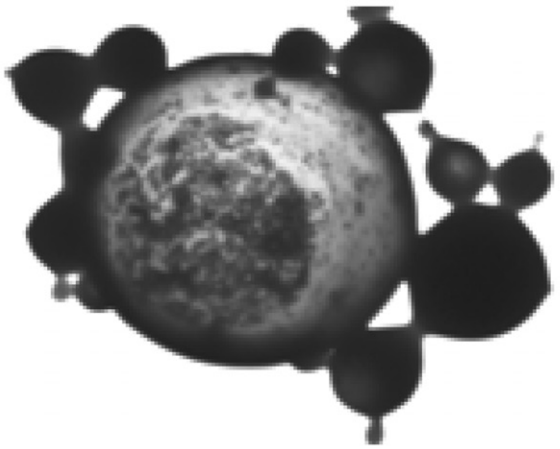

Figure 10. TEM photomicrograph of microparticles, showing the distribution of the SPIONs inside the polymer matrix; scale bar represents 10 μm.

DXM release

DXM release is a critical parameter in view of a medical application. For future intra-articular delivery, one aims at achieving DXM release over a few days.

The DXM release profile of the Batch 22 is presented in Figure 11. DXM is gradually released over approximatively a week, with a faster release in the first 24 h. These results are adequate for the *in vivo* applications in perspective.

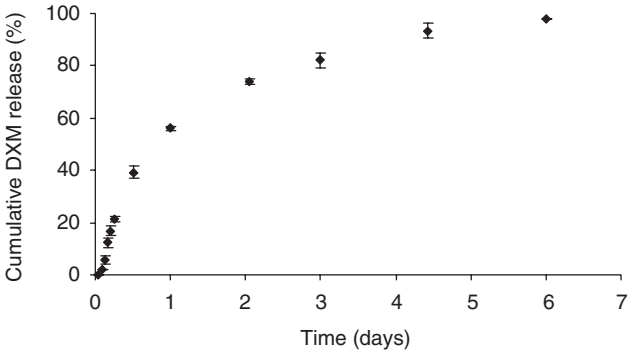

Figure 11. The DXM release profile of the Batch 22.

In order to be able to compare the release profiles of the 10 different batches of the full factorial design, the release of the DXM at 24 and 48 h was determined. As depicted in Figure 12(a), all batches released more then 50% of the active substance within 24 h.

Moreover, a relationship between DXM release profile and microparticle size or DXM loading can be established. In fact, the larger the microparticle size or the smaller the DXM loading, the slower the DXM release (Figure 12(b)), with a correlation coefficient of 0.83 and 0.6, respectively. The explanation for a slower drug release out of coarser microparticles can be found in the fact that the latter, compared to fine microparticles, are associated with a higher PLGA concentration in the organic phase and thus with a higher PLGA:DXM ratio (300:10 vs 200:10).

The molecular weight of the polymer alone and of the polymer inside the microparticles before and after 6 days of release was determined by GPC and the results do not show significant differences between the three measures (results not shown). As the polymer does not degrade during release testing, one can assume that DMX is released through a diffusion-controlled process. In order to explain the variations of the release kinetics with microparticle size and with DXM loading, two assumptions were made: (i) both the coarse and the fine microparticles have similar internal structures and (ii) DXM is homogeneously distributed inside of the microparticles. Under these conditions, it can be anticipated that DXM will diffuse more slowly in the dense matrix (high polymer:drug ratio) of the coarser microparticles. This conclusion is also supported by the fact that in the coarser microparticles the diffusion distance is larger than in the fine ones and thus the microparticle size is a determinant factor for the DXM release rate, as demonstrated also by Berkland et al. (2002).

From Figure 12(a), it can be inferred that experiment 6, which meets the specifications from the point of view of DXM loading and DXM encapsulation efficacy, in terms of desirability function, is not an interesting candidate for future medical applications, as DXM is almost 100% released after 24 h.

Furthermore, examination of the DXM release of the 10 batches of the full factorial design at 24 and 48 h

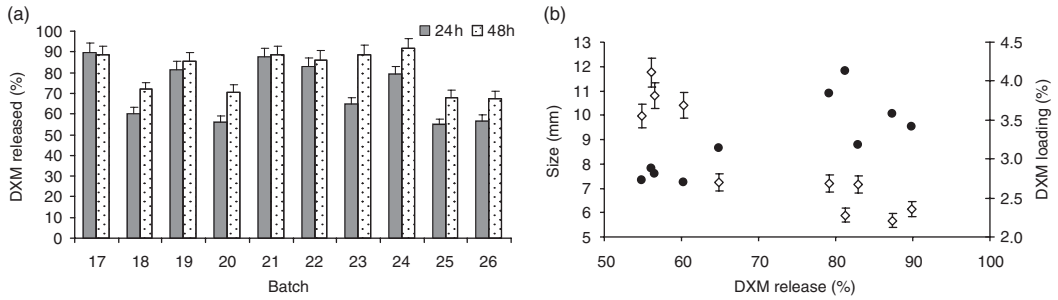

Figure 12. Percentage released of DXM after 24 and 48 h (a); Released DXM at 24 h as a function of microparticle size and DXM loading (b).

allowed one to highlight that the two favourable aspects for a slow diffusion are: (i) a more abundant polymer quantity in the microparticle matrix, thus in the organic phase, concomitant to (ii) a smaller DXM loading. From that, one can conclude that good candidates for future clinical applications are the experiments for which the PLGA concentration in the organic phase is $300\,mg\,ml^{-1}$. So, corroborating the DXM release profile of the batches with the specifications fixed for the microparticles in terms of DXM loading, DXM encapsulation efficacy and microparticle size, it can be concluded that the most interesting candidates for medical applications are Batches 18, 20, 25 and 26 of the full factorial design. It is noteworthy to emphasize that these batches fulfil the requirements in terms of microparticle size, DXM loading and DXM encapsulation efficacy as well.

Conclusion

To the authors' knowledge, up to date there are no reports of microparticles embedding two active substances: one dissolved in the polymer matrix and having a therapeutic effect and the other one as a suspension in the polymer matrix and having the role of keeping the whole system in place, with an external magnetic field.

The experimental design approach allowed one to find the best technological conditions leading to biodegradable microparticles of $\sim$10 µm, encapsulating both DXM and SPIONs. DXM was efficiently encapsulated into the microparticles with a drug loading suitable for future intra-articular applications. Moreover, SPIONs were also successfully encapsulated, resulting in magnetic retention of almost 100% of microparticles after 10 min under a 0.8 T magnetic field. This is a key issue for the *in vivo* application that is planned for the microparticles, demonstrating that they could be restrained in a specific site, notably into the joint, with an external magnetic field.

This study outlined the significance of parameters, such as PLGA concentration, stirring speed during solvent extraction and extractive volume on the particle formulation process.

A more thorough physical characterization of the microparticles is ongoing, focusing on the inner structure of the microparticles and SPION properties. *In vivo* experiments are also planned to demonstrate the approach of the magnetic retention to deliver an anti-inflammatory drug to the joint.

Acknowledgements

The authors would like to express their gratitude to Mrs Nathalie Boulens and Mrs Catherine Siegfried for assistance with the SEM, to Dr Christopher Bauer for performing the TEM analysis and to Mr Marcel Duerggelin for the SEM images of the inner structure of the microparticles. Dr Serge Rudaz is also kindly acknowledged for his constructive suggestions and advice in the analysis of the experimental designs. The authors are also grateful to Dr Cém Gabay and Dr Pierre-André Guerne for helpful discussion.

Declaration of interest: The authors report no conflicts of interest. The authors alone are responsible for the content and writing of the paper.

References

Beck RCR, Pohlmann AR, Hoffmeister C, Gallas MR, Collnot E, Schaefer UF, Guterres SS, Lehr CM. 2007. Dexamethasone-loaded nanoparticle-coated microparticles: Correlation between *in vitro* drug release and drug transport across Caco-2 cell monolayers. Eur J Pharm Biopharm 67:18–30.

Berkland C, King M, Cox A, Kim K, Pack DW. 2002. Precise control of PLG microsphere size provides enhanced control of drug release rate. J Contr Rel 82:137–147.

Bozdag S, Calis S, Kas HS, Ercan MT, Peksoy I, Hincal AA. 2001. *In vitro* evaluation and intra-articular administration of biodegradable microspheres containing naproxen sodium. J Micoencapsulation 18:443–456.

Cheng J, Teply BA, Jeong SY, Yim CH, Ho D, Sherifi I, Jon S, Farokhzad OC, Khademhosseini A, Langer RS. 2006. Magnetically responsive polymeric microparticles for oral delivery of protein drugs. Pharm Res 23:557–564.

Chastellain M, Petri A, Hofmann H. 2004. Particle size investigations of a multistep synthesis of PVA coated superparamagnetic nanoparticles. J Coll Interf Sci 278:353–360.

Gaffney K, Ledingham J, Perry JD. 1995. Intra-articular triamcinolone hexacetonide in knee osteoarthritis: Factors influencing the clinical response. Ann Rheum Dis 54:379–381.

Gerwin N, Hops C, Lucke A. 2006. Intraarticular drug delivery in osteoarthritis. Adv Drug Deliv Rev 58:226–242.

Ghassabian S, Ehtezazi T, Forutan SM, Mortazavi SA. 1996. Dexamethasone-loaded magnetic albumin microspheres: Preparation and *in vitro* release. Int J Pharm 130:49–55.

Gomez-Gaete C, Tsapis N, Besnard M, Bochot A, Fattal E. 2007. Encapsulation of dexamethasone into biodegradable polymeric nanoparticles. Int J Pharm 331:153–159.

Hamoudeh M, Faraj AA, Canet-Soulas E, Bessueille F, Leonard D, Fessi H. 2007. Elaboration of PLLA-based superparamagnetic nanoparticles: Characterization, magnetic behaviour study and *in vitro* relaxivity evaluation. Int J Pharm 338:248–257.

Horisawa E, Hirota T, Kawazoe S, Yamada J, Yamamoto H, Takeuchi H, Kawashima Y. 2002a. Prolonged anti-inflammatory action of DL-lactide/glycolide copolymer nanospheres containing betamethasone sodium phosphate for intra-articular delivery system in antigen-induced arthritic rabbit. Pharm Res 19:403–410.

Horisawa E, Kubota K, Tuboi I, Sato K, Yamamoto H, Takeuchi H, Kawashima Y. 2002b. Size-dependency of DL-lactide/glycolide copolymer particulates for intra-articular delivery system on phagocytosis in rat synovium. Pharm Res 19:132–139.

Hu FX, Neoh KG, Kang ET. 2006. Synthesis and *in vitro* anti-cancer evaluation of tamoxifen-loaded magnetite/PLLA composite nanoparticles. Biomaterials 27:5725–5733.

Khan MA, Sastry SV, Vaithiyalingam SR, Agarwal V, Nazzal S, Reddy IK. 2000. Captopril gastrointestinal therapeutic system coated with cellulose acetate pseudolatex: Evaluation of main effects of several formulation variables. Int J Pharm 193:147–156.

Kopp AF, Laniado M, Dammann F, Stern W, Gronewaller E, Balzer T, Schimpfky C, Claussen CD. 1997. MR imaging of the liver with Resovist: Safety, efficacy, and pharmacodynamic properties. Radiology 204:749–756.

Liggins RT, Cruz T, Min W, Liang L, Hunter WL, Burt HM. 2004. Intra-articular treatment of arthritis with microsphere formulations of paclitaxel: Biocompatibility and efficacy determinations in rabbits. Inflamm Res 53:363–372.

Metselaar JM, van den, Berg W, Holthuysen AEM, Wauben MHM, Storm G, van Lent PLEM. 2006. Liposomal targeting of glucocorticoids to synovial lining cells strongly increases therapeutic benefit in collagen type II arthritis. Ann Rheum 63:348–353.

Moore GF. 2005. Arthrocentesis technique and intraarticular therapy. In: Koopman WJ, Moreland LW, editors. Arthris and allied conditions—A textbook of rheumatology. Philadelphia: Lippincott Williams & Wilkins. pp 775–785.

Okassa LN, Marchais H, Douziech-Eyrolles L, Hervé K, Cohen-Jonathan S, Munnier E, Sourcé M, Linasssier C, Dubois P, Chourpa I. 2007. Optimization of iron oxide nanoparticles encapsulation within poly(D,L-lactide-co-glycolide) submicron particles. Eur J Pharm Biopharm 67:31–38.

Pean JM, Venier-Julienne MC, Filmon R, Sergent M, Phan-Tan-Luu R, Benoit JP. 1998. Optimization of HSA and NGF encapsulation yields in PLGA microparticles. Int J Pharm 166:105–115.

Ratcliffe JH, Hunneyball IM, Smith A, Wilson CG, Davis SS. 1987. Preparation and evaluation of biodegradable polymeric systems for the intra-articular delivery of drugs. J Pharm Pharmacol 36:431–436.

Raynauld J-P, Buckland-Wright C, Ward R, Choquette D, Haraoui B, Martel-Pelletier J, Uthman I, Khy V, Tremblay J, Bertrand C, Martel-Pelletier J. 2003. Safety and efficacy of long-term intraarticular steroid injections in osteoarthritis of the knee. A randomized, double-blind, placebo-controlled trial. Arthritis Rheum 48:370–377.

Schulze K, Koch A, Schopf B, Petri A, Steitz B, Chastellain M, Hofmann M, Hofmann H, von Rechenberg B. 2005. Intraarticular application of superparamagnetic nanoparticles and their uptake by synovial membrane–an experimental study in sheep. J Magn Magn Mater 293:419–432.

Timko M, Koneracka M, Tomasovicova N, Kopcansky P, Zavisova V. 2006. Magnetite polymer nanospheres loaded by Indomethacin for anti-inflammatory therapy. J Magn Magn Mater 300:e191–e194.

Tosu T. 1992. Steroid induced arthropathy. J Joint Surg 11:87–95.

Tuncay M, Calis S, Kas HS, Ercan MT, Peksoy I, Hincal AA. 2000. Diclofenac sodium incorporated PLGA (50:50) microspheres: Formulation considerations and *in vitro*/*in vivo* evaluation. Int J Pharm 195:179–188.

Weissleder R, Stark DD, Engelstad BL, Bacon BR, Compton CC, White DL, Jacobs P, Lewis J. 1989. Superparamagnetic iron oxide: Pharmacokinetics and toxicity. Am J Roentgenol 152:167–173.

Yang J, Park SB, Yoon HG, Huh YM, Haam S. 2006. Preparation of poly ε-caprolactone nanoparticles containing magnetite for magnetic drug carrier. Int J Pharm 324:185–190.

Zavisova V, Koneracka M, Strbak O, Tomasovicova N, Kopcansky P, Timko M, Vavra I. 2007. Encapsulation of indomethacin in magnetic biodegradable polymer nanoparticles. J Magn Magn Mater 311:379–382.